Indonesian Review of Physics (IRiP)
Vol.5, No.2, December 2022, pp. 66 - 72

p-ISSN: 2621-3761 | e-ISSN: 2621-2889
DOI: 10.12928/irip.v5i2.6706

Utilization of Seismic Data as a Tsunami Vulnerability Review

Azmi Khusnani[1]*, Adi Jufriansah[2], and Mulya Afriyanto[3]
[1,2] IKIP Muhammadiyah Maumere, Indonesia
[3] Meteorological, Climatological, and Geophysical Agency (BMKG), Sikka District, Indonesia
Email: husnaniazmi@gmail.com

Article Info

Article History
Received: Oct 10, 2022
Revision: Dec 23, 2022
Accepted: Dec 29, 2022

Keywords:
Bathymetry
Flores Sea
Run-Up
Tsunami
Vulnerability Level

ABSTRACT

This study aimed to analyze seismic data, which is then made into an infographic to map the level of tsunami hazard in the Sikka District. The research was carried out in Sikka District, East Nusa Tenggara, located between 121°55'40"-122°41'30" east longitude and 08°22'-08°50' south latitude. The data source comes from the IRIS Earthquake Browser, and the analysis stage was carried out in two phases. The first analysis used seismic data analysis, and EQ Energy used IRIS (Incorporated Research Institutions for Seismology) data. Meanwhile, the second analysis maps the tsunami risk by determining the tsunami hazard in areas with the potential for a tsunami. Based on the analysis of seismicity data showed that Sikka District has the potential for an earthquake accompanied by a tsunami. In contrast, the results of the EQ Energy analysis caused by the December 14, 2021 earthquake were known as the value of $E_{hf} = 6.46 \times 10^{14}$ J and $E_{BB} = 5.48 \times 10^{15}$ J. The analysis of the level of tsunami susceptibility based on the tsunami run-up height in Sikka District showed that the northern coastal area of Flores had various potentials, where the highest vulnerability level was in the Alok subdistrict and parts of Talibura. Meanwhile, the area with the lowest potential was the Kewapante subdistrict.

To cite this article:
A. Khusnani, A. Jufriansah, and M. Afriyanto, “Utilization of Seismic Data as a Tsunami Vulnerability Review,” *Indones. Rev. Phys.*, vol. 5, no. 2, pp. 66–72, 2022, doi: 10.12928/irip.v5i2.6706.

I. Introduction

Eastern Indonesia has a very dynamic region in its geological setting. It is caused by the eastern part of Indonesia being dominated by many islands separated by the deep sea. Another factor is the influence of the interaction of the three Indo-Australian, Eurasian and Pacific plates [1]. This geological location is the reason why Eastern Indonesia has many sources of seismic and non-seismic tsunamis [2], [3]. However, this differs from the region's seismic research [4], where the study mainly exposes western Indonesia [2], [5], [6].

Flores Island, located in East Nusa Tenggara, is one of the islands in Eastern Indonesia included in the Pacific Ring of Fire which shows high tectonic activity. It is due to the Flores thrust zone, which extends from northern Flores past Bali to West Nusa Tenggara [7], [8]. It is in line with a study conducted by Maneno *et al.* [4] revealed that the Flores region has the potential for tectonic earthquakes and generates tsunamis. The earthquake catalog noted that Flores was hit by an earthquake and tsunami with Mw > 7 in 1992 [9]. Okal [10] explains that the 1992 Flores earthquake and tsunami were caused by an underwater landslide and resulted in an extreme run-up as high as 26 m. Pranantyo and Cummins [11] added that this phenomenon causes a change in ground level with a lift of 1.1 m and a drop of -1.6 m. The results of field observations explained that after the tsunami occurred, there were no traces of buildings found on Babi Island, Flores [12], and the destruction of most of the north coast of Flores. This phenomenon also caused 1,952 dead and

500 people to go missing [13]. Other findings revealed that the damage caused by tsunami waves came from two directions with different magnitudes and deposited sand on the North and South coast [14].

The disaster that occurred in 1992 was destructive. Progress in tsunami research is that there has been a decrease in the number of victims affected [15]. However, the tsunami warning system has not been able to reduce the number of victims affected by the tsunami. Therefore, carrying out a tsunami risk assessment is crucial, especially in coastal areas [16]. A tsunami risk assessment can be in the form of conducting a tsunami risk mapping. Sengaji and Nababan [17] conducted tsunami risk mapping using earthquake distribution data from 1900 to 2007. However, on December 14, 2021, BMKG (Badan Meteorology, Climatology, and Geophysics) noted that an earthquake with an earthquake of Mw 7.4 scale occurred, which resulted in a small tsunami with a height of 7 cm [18]. Due to the Flores area's significant potential for earthquakes and tsunamis, it is necessary to update the analysis of the vulnerability level. The current results are expected to be used as a reference input for stakeholders in disaster mitigation. Based on the description above, the purpose of this study is to analyze seismic data, which is then made into an infographic to map the level of tsunami hazard in Sikka District.

II. Theory

Flores Earthquake Review

Based on geological data, Handayani [9] explained that Flores Island is in an active tectonic area, where several plate boundaries bound the region. The plate boundary in the area is the eastern end of the subduction of the Indo-Australian plate towards Eurasia, with the plate length extending from Java to Sumatra. The Australian continental plate and the Banda plate collide at the western boundary. The northern coastal area of Flores Island (as per Figure 1) is the Flores back thrust that extends along the island and is connected to the Wetar Thrust in the east.

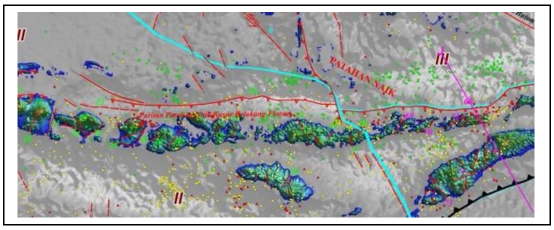

Figure 1. Active fault in Flores Island (https://geologi.esdm.go.id/geomap/)

Based on the study of earthquake history over 30 years, two earthquakes had Mw > 7. On December 12, 1992, an earthquake with an Mw of 7.8 occurred near Babi Island. People in the eastern half of Flores Island and the surrounding islands can feel the earthquake. In addition to an earthquake with a large magnitude, this earthquake caused a tsunami with inundation reaching a distance of 30 m to the west, a depth of 20.4 km, and a run-up measured at Ilepadung – East Flores of 11 m, Babi Island, Sikka District 5.5 m, and Wuring - Sikka 2.4 m [13]. The next earthquake occurred on December 14, 2021, in Flores with a strike-slip mechanism causing a new fault [19]. If tracing the past earthquake (50 years) in the area, there was an earthquake in 1997 with Mw 8.3 and 1995 with Mw 6.5.

Based on the previous description, Wiens [20] explained that a giant earthquake that occurs will be accompanied by aftershocks, which are related to changes in the polarity of the displacement waveform. Meanwhile, another explanation was put forward by Goes *et al.* [21] the fault mechanism changes in the mainshock and aftershock, caused by the strike-slip component of the mainshock consistent with the clockwise rotation of the slab material in an east-west direction to north-south.

The study's results follow the surface structure modeling in Figure 2 [22]. The modeling in Figure 3 corresponds to Setiadi [23]. The relocation results showed a significant decrease in the hypocenter to the north of about 640 km. He found a gap of earthquake activity along the subduction plate at the hypocenter of 300 - 400 km due to the partial melting of rocks in the mantle layer.

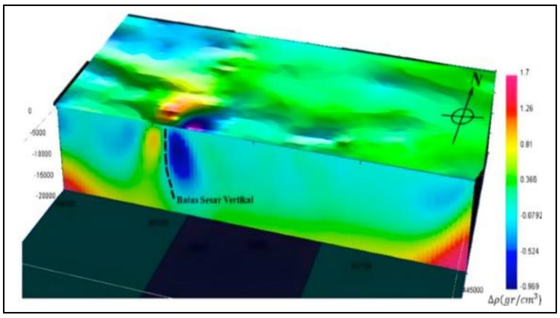

Figure 2. 3D modeling of subsurface structures in the region [22]

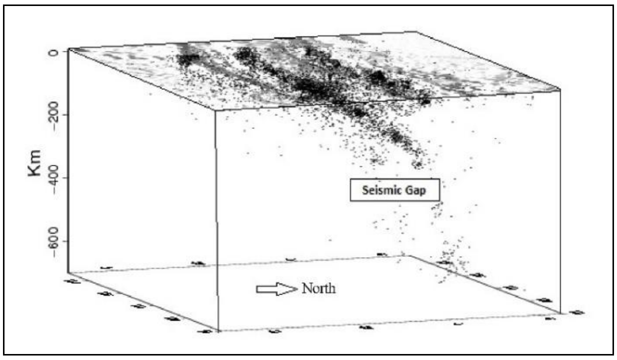

Figure 3. Image of a three-dimensional model of the relocation of Teletomo DD [23]

Tsunami

A tsunami is a series of ocean waves with a large wavelength. Tsunamis occur due to the movement of a substantial volume of water. This event can be caused by an earthquake or ground shaking in the sea [24]. In addition, a tsunami can be characterized by a sudden drop

p-ISSN: 2621-3761
e-ISSN: 2621-2889

in sea level followed by a substantial increase in seawater volume towards the coast and a vertical tsunami [25].

Tsunami disasters can sometimes be global, originating from one place and destructive at a distance of thousands of kilometers from the source. If you trace the history of the tsunami that occurred, it can be seen that the process of tsunami occurrence has different events based on the cause of its occurrence.

Tsunami Run-up

Tsunami run-up is the height of sea water waves calculated from the absolute limit of tsunami wave inundation from the zero point of sea level or mean sea level. The run-up height and tsunami height depend on the earthquake magnitude, seafloor morphology, and the shape of the coast. The magnitude of an earthquake affects the energy that causes a tsunami. Therefore, the upper run-up limit is an important parameter to determine the beach profile. Difficulties that are often encountered when predicting run-up are sea wave transformation and wave reflection. Land run-up speed can reach 25-100 km/h. The return of water to the sea after reaching the wave crest (run down) is also destructive because it drags everything back into the sea [26].

When the tsunami approaches the shoreline/land, the shallow part of the seabed serves to break or reduce the bottom wave propagation speed. Therefore, the closer you get to the beach, the slower the speed of the lower sea waves, while the speed of the upper waves is still high, the higher the sea wave height or amplitude and the shorter the wavelength. Likewise, the faster the friction between the waves and the beach bottom, the slower the bottom wave propagation speed, but the higher the maximum wave amplitude (run-up) will be greater.

III. Method

The research was carried out in Sikka District, East Nusa Tenggara, which is located between 121°55'40"-122°41'30" east longitude and 08°22'-08°50' south latitude. The earthquake data was used on December 14, 2021, using data from the IRIS (Incorporated Research Institutions for Seismology) Earthquake Browser (https://ds.iris.edu/ieb/).

In the analysis stage, two stages are carried out. The first stage analyzes seismic data, and the second is EQ Energy. EQ Energy is the cumulative seismic energy released by an earthquake. The EQ Energy value was obtained using IRIS data. This analysis will focus on the cumulative energy growth of the earthquake impact. The following analysis is tsunami risk mapping by determining tsunami hazards in areas with the potential for a tsunami to occur. Tsunami-prone areas are mapped by mapping tsunami height point data or run-up analysis based on the data for the tsunami in Flores on December 14, 2021. The tsunami run-up analysis is beneficial to determine the area's vulnerability to the potential for a tsunami, with the criteria for exposure according to Table 1 [17].

IV. Results and Discussion

Seismic analysis of the Flores area

The Flores Sea area is seismically active, following Figure 4 shows seismicity data from 1970-2022 with Mw 5.0. Based on the earthquake's depth analysis during this period, the depth values varied from 0-33 km in purple to 800 km in red (Figure 4b). Seismicity studies say that the zone classification in the Flores region is divided into five parts. The category is the Flores back arc thrust zone in the north of the island with shallow to medium thrust, shallow and medium thrust zones in Timor Through, and intermediate depth thrusts in the Sawu Basin and normal in the east, between Sumbawa Island and Flores with strike-slip and subduction earthquakes [9], [27]. The new findings suggest that the Flores back arc thrust has extended along the southern boundary of the Java Sea from Alor in the east to East Java in the western Java Sea [11], [28].

Pranantyo *et al.* [2] pointed out that, in the Flores region, there had been a tsunami phenomenon in the pre-instrumental period (in 1815, 1818, 1820, and 1836) and the period after the 1992 pre-instrumental with Mw 7.8. This phenomenon relates to Flore's back arc thrust tectonic activity [2], [13].

In the earthquake phenomenon, the magnitude of the magneto plays a significant role in tsunami generation. It is because the emergence of an earthquake can be followed by other phenomena [29]. The reappearance of the December 14, 2021, earthquake has great potential to release energy. Based on BMKG data, the spectral acceleration analysis noted that the ground acceleration value based on the accelerograph sensor showed a variable value between 0.16 to 74.44 gals. The study results from the nearest station (LFTI), about 91.99 km from the earthquake's epicenter, recorded a maximum ground acceleration of 24.45 gals. However, compared with the IBTI seismic station, the ground acceleration of 74.44 gals can be felt in Ile Boleng, East Flores, with a distance from the epicenter of about 120.6 km. So, based on this analysis, it will impact the cumulative energy if it is reviewed based on the arrival time of the P wave (Figure 2).

Table 1. Relationship of tsunami run-up height, tsunami risk, and level of damage

Run-up height (m)	Damage	Risk level (R)	Scale
> 16	Very big	Very high risk	5
6-16	Big	Hight risk	4
2-6	Intermediate	Medium risk	3
0.75-2	Small	Low risk	2
< 0.75	Very small	Very low risk	1

The earthquake on December 14, 2021, with Mw 7.4, resulted in a small tsunami with a height of 7 cm [18]. When viewed based on the energy generated.

Figure 5 is the result of EQ Energy for Mw 7.3 Flores Sea by IRIS. Based on Figure 5 for the cumulative energy plot for earthquake data on December 14, 2021, it is determined that this phenomenon is at a high frequency of

p-ISSN: 2621-3761
e-ISSN: 2621-2889

0.5-2 s and a wideband range of 0.5-70 s. the black vertical line (91 s) represents the inflection point determined by the crossover between near-constant growth and high-frequency energy, then marks the approximate burst duration [30]. At this point, the cumulative energy is determined for high frequency (E_{hf} = 6.46 × 10^{14} J) and broadband (E_{BB} = 5.48 × 10^{15} J). The high-frequency energy values are equivalent and assume only 1/5 of the energy is available in the selected higher pass band.

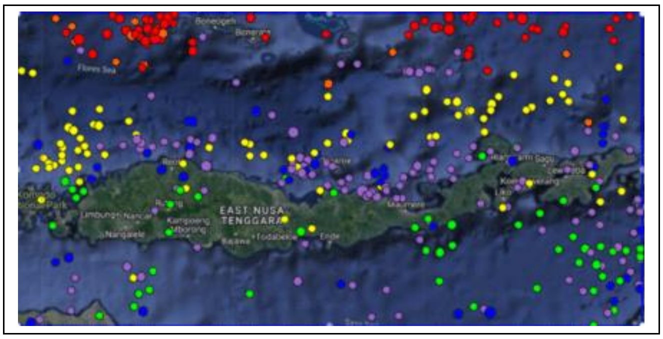

(a)

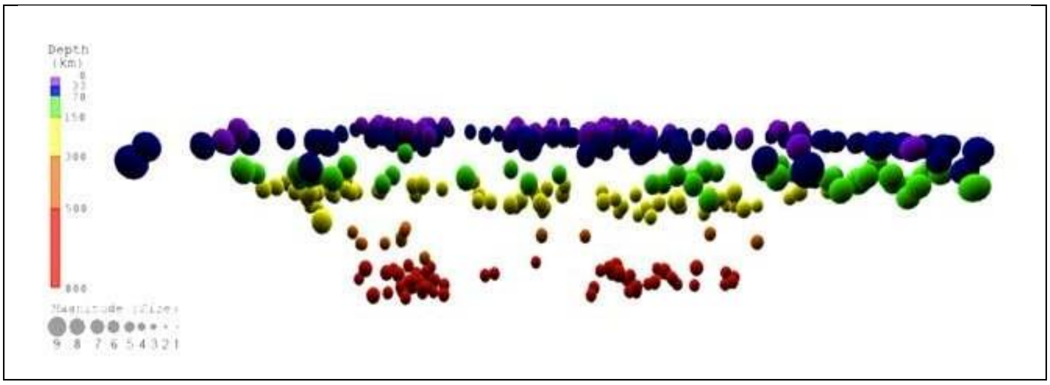

(b)

Figure 4. Seismic activity in the Flores region for the period 1970-2022, (a) distribution of seismic activity, and (b) distribution of earthquake activity based on depth and magnitude

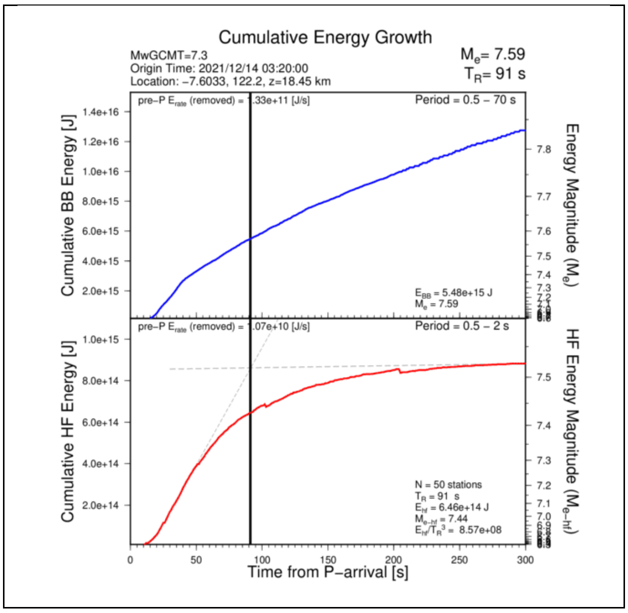

Figure 5. EQ Energy for Mw 7.3 Flores Sea

p-ISSN: 2621-3761
e-ISSN: 2621-2889

While Figure 6 is a hemispheric visualization event that is taken regularly at a distance of 25 degrees to 80 degrees. It is done to avoid triplication and energy bias calculations when there is a dense collection of stations. It is taken from the initial station collection using a minimum distance between stations of 5 degrees sampled from available broadband stations.

The seismicity data analysis shows that Sikka District has the potential for an earthquake accompanied by a tsunami; this can be seen in the 1992 Flores earthquake, with the most severely affected area in Maumere, Sikka District. It is crucial to map tsunami-prone locations. Common mistakes include subscripts; for instance, the quant.

Analysis of the tsunami hazard level of Sikka District

Determination of the level of tsunami susceptibility aims to determine the potential tsunami area. Figure 7 is a map of the tsunami hazard area in the Sikka District. The area's vulnerability level to possible tsunami is in Table 1, where high vulnerability with run-up > 6-16 m is in the Alok subdistrict and part of the Talibura subdistrict. Furthermore, moderate exposure with run-up height > 2-6 m covers almost the entire northern coastal area, namely the Magepanda subdistrict, Alok subdistrict, Waigete subdistrict, and Talibura subdistrict. Meanwhile, the lowest vulnerability with run-up > 0.75-2 m is in the Kewapante subdistrict.

The coastal area is an area that is directly nearby the sea and has the potential to be affected by a tsunami [31]. The high level of vulnerability in Figure 7 indicates that the area has a high potential for a tsunami. Based on the analysis results, it can be claimed that the overall vulnerability level of the Sikka District is low; this is because the Sikka District area is dominated by hilly regions (Figure 8). However, many people live in coastal areas. For example, in the 1992 Flores tsunami phenomenon, it was found that most of the victims were in the Alok subdistrict, where the population lives in the Wuring and Beru areas, which coincide with the coastal areas with a very high vulnerability level (Figure 9).

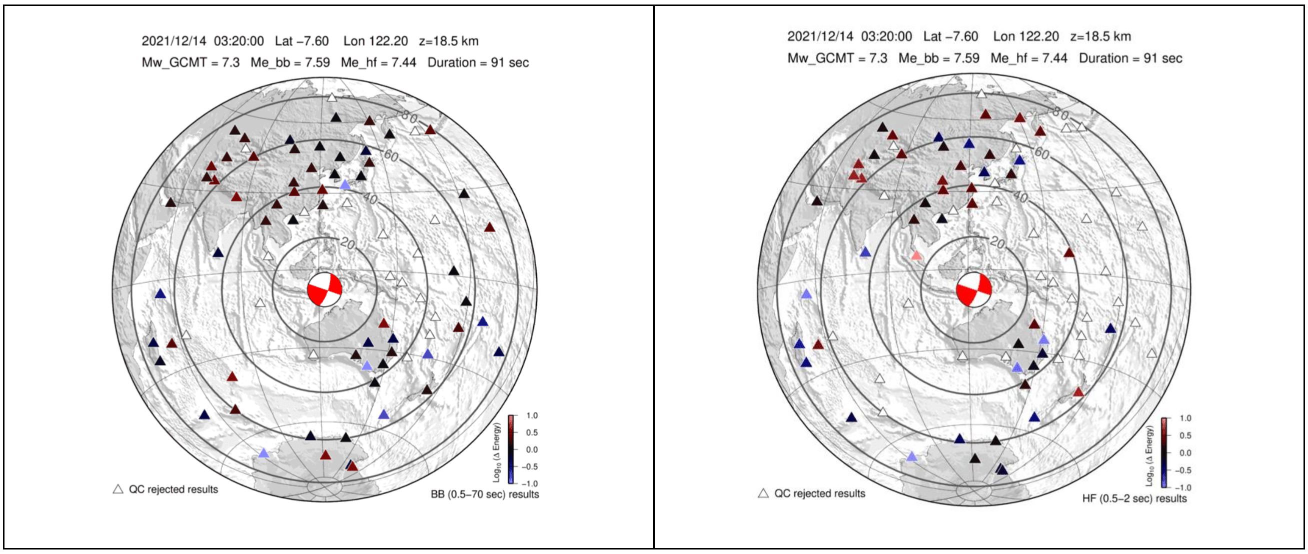

(a) (b)

Figure 6. Hemispheric visualization, (a) BB (0.5-70 sec), and (b) HF (0.5-2 sec)

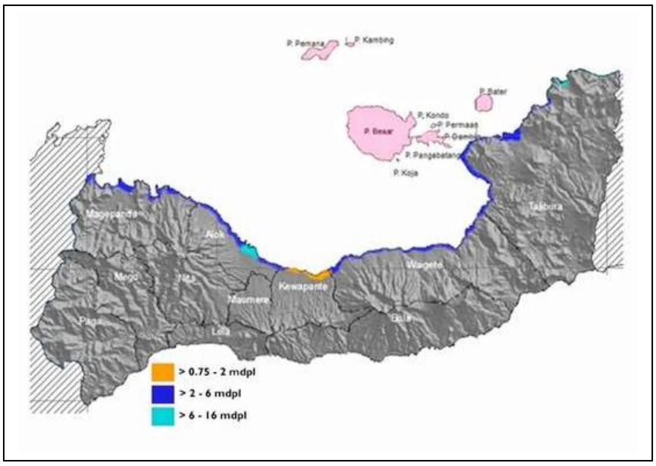

Figure 7. Tsunami hazard map based on tsunami run-up data for coastal areas

p-ISSN: 2621-3761
e-ISSN: 2621-2889

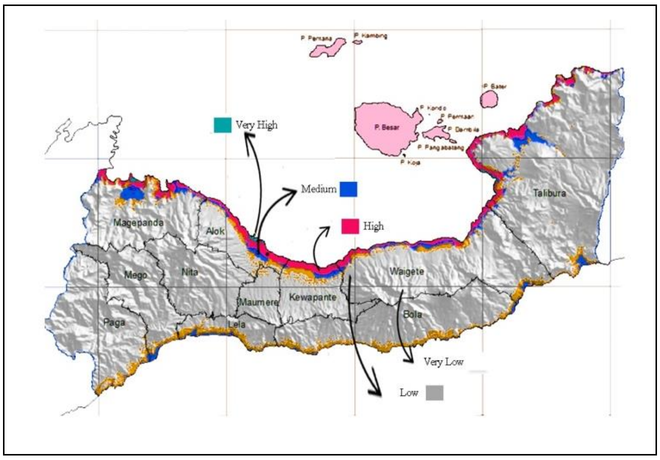

Figure 8. Tsunami hazard map of Sikka District

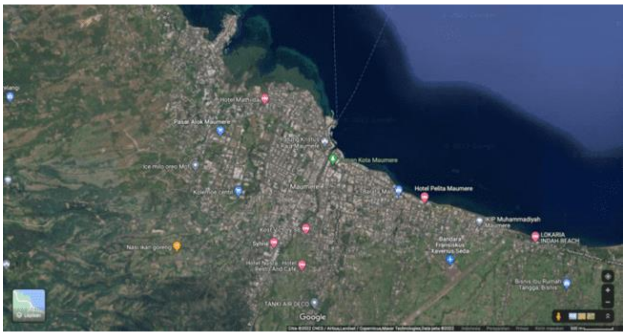

Figure 9. Map of settlements in the coastal area of Alok subdistrict (https://www.google.com/maps/)

V. Conclusion

The seismic data analysis shows that the Flores area has the potential for earthquakes with tsunamis, which is indicated by the number of earthquakes with a scale of Mw 5 from 1970-2022. It plays a critical role in tsunami generation. In addition, the Flores Sea has a history of earthquakes accompanied by tsunamis from the pre-instrumental period and after the pre-instrumental period. Based on the EQ Energy analysis caused by the December 14, 2021 earthquake, it is known that the value of $E_{hf} = 6.46 \times 10^{14}$ J and $E_{BB} = 5.48 \times 10^{15}$ J. Furthermore, the analysis of the level of tsunami vulnerability based on the tsunami run-up height in Sikka District indicates that the coastal area of the northern coast of Flores has diverse potential, with the highest level of exposure in the subdistrict of Alok and parts of Talibura. Meanwhile, the area with the lowest potential is in the Kewapante subdistrict. There is a potential for a tsunami on the north sea coast of Flores, so research on simulating inundation due to a tsunami will be very supportive as a mitigation effort.

VI. Acknowledgment

The researcher would like to thank the Indonesian Ministry of Education, Culture, Research and Technology for providing research funds through the 2022 Beginner Lecturer Research Grant Scheme (PDP).

References

[1] H. Kurnio, T. Naibaho, and C. Purwanto, "Review of Submarine Landslides in the Eastern Indonesia Region," *Bull. Mar. Geol.*, vol. 34, no. 2, pp. 63–76, Dec. 2019, doi: 10.32693/bomg.34.2.2019.618.

[2] I. R. Pranantyo, M. Heidarzadeh, and P. R. Cummins, "Complex Tsunami Hazards in Eastern Indonesia from Seismic and Non-Seismic Sources: Deterministic Modelling Based on Historical and Modern Data," *Geosci. Lett.*, vol. 8, no. 1, p. 20, Dec. 2021, doi: 10.1186/s40562-021-00190-y.

[3] K. Sinki, Y. Fujii, and B. Shibazaki, "Numerical Simulations of the 1992 Flores Tsunami," 2021. [Online]. Available: https://iisee.kenken.go.jp/syndb/data/20211209487648b2.pdf.

[4] R. Maneno, B. J. Sentosa, and G. Rachman, "Relocation of Earthquake Hypocenter in the Flores Region Using Hypo71," *IPTEK J. Eng.*, vol. 5, no. 2, pp. 33–37, May 2019, doi: 10.12962/j23378557.v5i2.a5024.

[5] A. Muhammad, K. Goda, N. A. Alexander, W. Kongko, and A. Muhari, "Tsunami Evacuation Plans for Future Megathrust Earthquakes in Padang, Indonesia, Considering Stochastic Earthquake Scenarios," *Nat. Hazards Earth Syst. Sci.*, vol. 17, no. 12, pp. 2245–2270, Dec. 2017, doi: 10.5194/nhess-17-2245-2017.

[6] I. E. Mulia, S. Watada, T. Ho, K. Satake, Y. Wang, and A. Aditiya, "Simulation of the 2018 Tsunami Due to the Flank Failure of Anak Krakatau Volcano and Implication for Future Observing Systems," *Geophys. Res. Lett.*, vol. 47, no. 14, pp. 1–9, Jul. 2020, doi: 10.1029/2020GL087334.

[7] R. P. Felix, J. A. Hubbard, K. E. Bradley, K. H. Lythgoe, L. Li, and A. D. Switzer, "Tsunami Hazard in Lombok and Bali, Indonesia, Due to the Flores Back-arc Thrust," *Nat. Hazards Earth Syst. Sci.*, vol. 22, no. 5, pp. 1665–1682, May 2022, doi: 10.5194/nhess-22-1665-2022.

[8] A. Koulali *et al.*, "Crustal Strain Partitioning and the Associated Earthquake Hazard in the Eastern Sunda-Banda Arc," *Geophys. Res. Lett.*, vol. 43, no. 5, pp. 1943–1949, Mar. 2016, doi: 10.1002/2016GL067941.

[9] L. Handayani, "Seismic Hazard Analysis of Maumere, Flores: a Review of the Earthquake Sources," 2020, doi: 10.4108/eai.12-10-2019.2296247.

[10] E. A. Okal, "Twenty-Five Years of Progress in the Science of 'Geological' Tsunamis Following the 1992 Nicaragua and Flores Events," *Pure Appl. Geophys.*, vol. 176, no. 7, pp. 2771–2793, Jul. 2019, doi: 10.1007/s00024-019-02244-x.

[11] I. R. Pranantyo and P. R. Cummins, "Multi-Data-Type Source Estimation for the 1992 Flores Earthquake and Tsunami," *Pure Appl. Geophys.*, vol. 176, no. 7, pp. 2969–2983, Jul. 2019, doi: 10.1007/s00024-018-2078-4.

[12] K. O. Kim, D. C. Kim, J.-H. Yuk, E. Pelinovsky, and B. H. Choi, "Extreme Tsunami Inundation at Babi Island due to Flores Earthquake Induced Tsunami in 1992," *Ocean Polar Res.*, vol. 37, no. 2, pp. 91–105, Jun. 2015, doi:

10.4217/OPR.2015.37.2.091.

[13] A. M. Julius and Daryono, "Overview of 1990s Deadly Tsunamis in Indonesia," *E3S Web Conf.*, vol. 331, p. 07001, Dec. 2021, doi: 10.1051/e3sconf/202133107001.

[14] K. Minoura, F. Imamura, T. Takahashi, and N. Shuto, "Sequence of Sedimentation Processes Caused by the 1992 Flores Tsunami: Evidence from Babi Island," *Geology*, vol. 25, no. 6, pp. 523–526, 1997, doi: 10.1130/0091-7613(1997)025<0523:SOSPCB>2.3.CO;2.

[15] U. Kânoğlu, Y. Tanioka, E. A. Okal, M. A. Baptista, and A. B. Rabinovich, "Introduction to 'Twenty Five Years of Modern Tsunami Science Following the 1992 Nicaragua and Flores Island Tsunamis, Volume II,'" *Pure Appl. Geophys.*, vol. 177, no. 3, pp. 1183–1191, Mar. 2020, doi: 10.1007/s00024-020-02451-x.

[16] N. Cabral, "Revision of the Azorean Catalogue of Tsunamis," *Geol. Soc. London, Spec. Publ.*, vol. 501, no. 1, pp. 301–325, Jan. 2021, doi: 10.1144/SP501-2019-107.

[17] E. Sengaji and B. Nababan, "Pemetaan Tingkat Resiko Tsunami di kabupaten Sikka, Nusa Tenggara Timur," *J. Ilmu dan Teknol. Kelaut. Trop.*, vol. 1, no. 1, pp. 48–61, Jul. 2009, doi: 10.29244/jitkt.v1i1.7938.

[18] Badan Geologi, "Analisis Geologi Kejadian Gempa Bumi Merusak Di Laut Flores, Tanggal 14 Desember 2021," *Kementerian Energi dan Sumber Daya Mineral*, 2021. https://vsi.esdm.go.id/index.php/gempabumi-a-tsunami/kejadian-gempabumi-a-tsunami/3868-analisis-geologi-kejadian-gempa-bumi-merusak-di-laut-flores-tanggal-14-desember-2021.

[19] P. Supendi *et al.*, "The Kalaotoa Fault: A Newly Identified Fault that Generated the Mw 7.3 Flores Sea Earthquake," *Seism. Rec.*, vol. 2, no. 3, pp. 176–185, Jul. 2022, doi: 10.1785/0320220015.

[20] D. A. Wiens, "Source and Aftershock Properties of the 1996 Flores Sea Deep Earthquake," *Geophys. Res. Lett.*, vol. 25, no. 6, pp. 781–784, Mar. 1998, doi: 10.1029/98GL00417.

[21] S. Goes, L. Ruff, and N. Winslow, "The Complex Rupture Process of the 1996 Deep Flores, Indonesia Earthquake (Mw 7.9) from Teleseismic P-waves," *Geophys. Res. Lett.*, vol. 24, no. 11, pp. 1295–1298, Jun. 1997, doi: 10.1029/97GL01245.

[22] A. K. Maimuna, A. F. Miftakhunnisa, and Y. A. Segoro, "Pemodelan Inversi 3 Dimensi untuk Identifikasi Dugaan Keberadaan Sesar menggunakan Data Anomali Gaya Berat di Laut Flores (Studi Kasus Gempa Flores 14 Desember 2021)," *Prog. J. Geofis.*, vol. 1, no. 1, pp. 55–62, 2022, [Online]. Available: https://jurnal.stmkg.ac.id/index.php/pjg/article/view/260.

[23] T. A. P. Setiadi, "Relokasi Gempabumi Teleseismic Double-Difference di Wilayah Bali – Nusa Tenggara dengan Model Kecepeatan 3D," *J. Lingkung. dan Bencana Geol.*, vol. 9, no. 1, pp. 45–52, Apr. 2018, doi: 10.34126/jlbg.v9i1.149.

[24] K. Nisa, L. Ambarwati, and T. Murdiyanto, "Simulasi Penjalaran Gelombang Tsunami Menggunakan Metode Optimal Time Stepping," *JMT J. Mat. dan Terap.*, vol. 3, no. 1, pp. 10–19, Feb. 2021, doi: 10.21009/jmt.3.1.2.

[25] P. Tandel, H. Patel, and T. Patel, "Tsunami Wave Propagation Model: A Fractional Approach," *J. Ocean Eng. Sci.*, vol. 7, no. 6, pp. 509–520, Dec. 2022, doi: 10.1016/j.joes.2021.10.004.

[26] I. P. A. Suriajaya Maha Putra, K. N. Suarbawa, and I. G. A. Putra Adnyana, "Studi Mitigasi Bencana Tsunami Dengan Menentukan Run Up Dan Waktu Tiba Tsunami Daerah Banyuwangi," *Bul. Fis.*, vol. 23, no. 2, pp. 130–136, Sep. 2022, doi: 10.24843/BF.2022.v23.i02.p08.

[27] I. R. Pranantyo and P. R. Cummins, "The 1674 Ambon Tsunami: Extreme Run-Up Caused by an Earthquake-Triggered Landslide," *Pure Appl. Geophys.*, vol. 177, no. 3, pp. 1639–1657, Mar. 2020, doi: 10.1007/s00024-019-02390-2.

[28] P. Supendi *et al.*, "Fate of Forearc Lithosphere at Arc-Continent Collision Zones: Evidence From Local Earthquake Tomography of the Sunda-Banda Arc Transition, Indonesia," *Geophys. Res. Lett.*, vol. 47, no. 6, p. e2019GL086472, Mar. 2020, doi: 10.1029/2019GL086472.

[29] U. Kânoğlu, Y. Tanioka, E. A. Okal, M. A. Baptista, and A. B. Rabinovich, "Introduction to 'Twenty Five Years of Modern Tsunami Science Following the 1992 Nicaragua and Flores Island Tsunamis, Volume I,'" *Pure Appl. Geophys.*, vol. 176, no. 7, pp. 2757–2769, Jul. 2019, doi: 10.1007/s00024-019-02266-5.

[30] G. L. Choy and J. L. Boatwright, "Global Patterns of Radiated Seismic Energy and Apparent Stress," *J. Geophys. Res. Solid Earth*, vol. 100, no. B9, pp. 18205–18228, Sep. 1995, doi: 10.1029/95JB01969.

[31] M. A. Marfai *et al.*, "Tsunami Hazard Mapping and Loss Estimation Using Geographic Information System in Drini Beach, Gunungkidul Coastal Area, Yogyakarta, Indonesia," *E3S Web Conf.*, vol. 76, p. 03010, Jan. 2019, doi: 10.1051/e3sconf/20197603010.

Declarations

Author contribution : Azmi Khusnani is responsible for the entire research project. He also leads scriptwriting and collaborations with other writers. Adi Jufriansah participated in data collection and analysis. Mulya Afriyanto participated as a data supplier. All authors approved the final manuscript.

Funding statement : This research is funded by the government of Indonesian Ministry of Education, Culture, Research and Technology with the contract no. 1098/LL15/KM/2022)

Conflict of interest : All authors declare that they have no competing interests.

Additional information : No additional information is available for this paper.

p-ISSN: 2621-3761
e-ISSN: 2621-2889